

Melting phase relation of Fe-bearing Phase D up to the uppermost lower mantle

**Chaowen Xu^{*1,2,3,4}, Toru Inoue^{1,5,6}, Jing Gao⁷, Masamichi Noda^{1,5,6}, Sho
Kakizawa^{1,5,6}**

¹ Geodynamics Research Center, Ehime University, 2-5 Bunkyo-cho, Matsuyama
790-8577, Japan

² Institute of Earthquake Forecasting, China Earthquake Administration (CEA,) Beijing,
China

³ The United Laboratory of High-Pressure Physics and Earthquake Science, China
Earthquake Administration (CEA,) Beijing, China

⁴ Key Laboratory of Earth and Planetary Physics, Institute of Geology and Geophysics,
Chinese Academy of Sciences, Beijing, China

⁵ Department of Earth and Planetary Systems Science, Hiroshima University, 1-3-1
Kagamiyama, Higashi-Hiroshima 739-8526, Japan

⁶ Hiroshima Institute of Plate Convergence Region Research (HiPeR), Hiroshima
University, Higashi-Hiroshima, Hiroshima 739-8526, Japan

⁷ State Key Laboratory of Lithospheric Evolution, and Institutions of Earth Science,
Institute of Geology and Geophysics, Chinese Academy of Sciences, Beijing, China

* Corresponding author: Chaowen Xu (dkchaowen@126.com)

Contents of this file

Text S1

Table S1

Figure S1

Text S1

In this following, we describe detailed experimental procedure to analyze the recovered samples after high P-T experiments:

The recovered run products were mounted in epoxy resin and were polished to perform phase identification and composition analysis. The phase assemblages were identified using a microfocus X-ray diffractometer (MicroMax-007HF; Rigaku Corp.), which is equipped with a rotative anode (Cu K α 1 radiation), a two-dimensional imaging plate detector, and ϕ 100- μ m collimator. The operating conditions were 40 kV and 30 mA, and exposure time for X-ray powder diffraction analyses was 600 s. Lattice parameters of PhD were calculated using six to eight peaks in a two-theta range from 15° to 80°. We used polycrystalline Si as an external standard to calibrate the peak positions of the X-ray powder diffraction patterns. The obtained data were processed by 2PD software, which can display and process two-dimensional data, including smoothing, background correction, and 2-D to 1-D conversion. Each 1-D X-ray profile was analyzed using the PDIndexer software (Seto et al., 2010). The samples were coated with carbon for electron microscopic observation and compositional analysis. The microtextures and compositions were obtained using a field emission scanning electron microscope (JSM7000F; JEOL) combined with an energy dispersive X-ray spectrometer (X-MaxN; Oxford Instruments plc.) with working parameters of 15 kV, 1 nA, and collection times of 30–50 s. The energy dispersive X-ray spectrometer data were processed by the software Aztec (Version 2.4, Oxford Instruments Nanotechnology Tools Ltd) using the XPP method.

Reference in the text

Seto, Y., Nishio-Hamane, D., Nagai, T., and Sata, N. (2010) Development of a software suite on X-ray diffraction experiments. *Review of High Pressure Science and Technology*, 20, 269–276.

Table S1. Chemical compositions (wt%) of typical coexisting phases (run a, 15.0 wt% αFeOOH + $\text{Mg}_{1.11}\text{Si}_{1.89}\text{O}_6\text{H}_{2.22}$; run b, 8.0 wt% αFeOOH + $\text{Mg}_{1.11}\text{Si}_{1.89}\text{O}_6\text{H}_{2.22}$; run c, pyrolite and MORB-type composition). Some of melt is not shown due to poor quality. Numbers in parentheses represent uncertainties.

Run	P (GPa)	T (°C)	EDS analysis number	Phase	MgO	SiO ₂	Fe ₂ O ₃	Total
a	25#	1600#	12	St	0	105.78(2.43)	0	105.78(2.43)
			1	Melt	31.43	27.40	20.99	79.82
		1400	14	Brg	36.89(0.42)	58.37(0.70)	7.32(0.58)	102.58(0.71)
			9	Fe ₂ O ₃	11.27(0.66)	0.76(0.36)	88.01(0.72)	100.04(0.91)
			11	St	0	100.78(0.81)	0.23(0.20)	101.01(0.77)
		1200	18	PhD	21.63(0.47)	61.32(0.47)	5.27(0.25)	88.22(0.77)
			13	Fe ₂ O ₃	6.89(1.82)	1.70(1.55)	90.46(1.77)	99.05(1.71)
			21	1300	16	Rw	44.00(0.68)	39.34(0.51)
	14	St			0	99.70(1.49)	0.52(0.07)	100.22(1.45)
	1100	25		PhD	22.91(1.50)	58.83(2.15)	4.93(0.74)	86.67(1.80)
		12		Fe ₂ O ₃	2.32(0.43)	0	99.09(2.22)	101.41(1.29)
	20	1100	24	PhD	20.72(0.37)	62.26(0.33)	5.38(0.17)	88.36(0.62)
			13	Fe ₂ O ₃	6.56(0.27)	0.25(0.18)	93.09(0.79)	99.90(0.61)
		18	1000	27	PhD	20.44(0.27)	61.70(0.84)	5.85(0.10)
	15			Fe ₂ O ₃	3.81(0.77)	0.79(0.62)	80.97(1.79)	94.57(1.16)
	1			Melt	15.9	51.41	6.66	73.97

Run	P (GPa)	T (°C)	EDS analysis number	Phase	MgO	SiO ₂	Fe ₂ O ₃	Total
b	25#	1600#	12	St	0	103.17(2.81)	0	103.17(2.81)
			1	Melt	36.15	27.75	13.12	77.01
		1400	14	Brg	38.04(0.26)	59.25(0.38)	4.58(0.42)	101.87(0.61)
			12	St	0	101.01(0.58)	0	101.01(0.58)
		1200	19	PhD	21.59(0.58)	60.59(0.59)	4.24(0.43)	86.42(0.77)
			13	Fe ₂ O ₃	8.27(0.83)	0.27(0.14)	89.27(0.26)	97.81(0.59)
	21	1300	17	Rw	46.99(0.35)	40.30(0.35)	13.01(0.14)	100.30(0.58)
			12	St	0	100.16(0.61)	0	100.16(0.61)
		1100	19	Rw	48.18(0.73)	41.05(0.46)	13.2(0.28)	102.43(0.30)
			26	PhD	21.79(0.79)	63.58(0.49)	3.82(0.36)	89.19(0.96)
			14	St	0	100.94(1.06)	0.42(0.08)	101.36(1.10)
	20	1100	16	Rw	42.28(0.32)	39.04(0.36)	19.32(0.24)	100.64(0.77)
			22	PhD	20.97(0.63)	62.69(1.13)	5.17(0.32)	88.83(1.74)
			13	St	0	98.89(1.56)	0	98.89(1.56)
	18	1000	26	PhD	20.27(0.34)	62.04(0.50)	5.23(0.26)	87.54(0.76)
			1	Melt	16.40	52.86	5.63	74.89

#Sample thermal fracturing when putting in oven, the surface is not smooth

Run	P (GPa)	T (°C)	EDS analysis number	Phase	MgO	Al ₂ O ₃	SiO ₂	Fe ₂ O ₃	Total
c									
MORB	21	1500	17	Gt	26.00(0.55)	22.07(0.99)	43.88(0.70)	8.49(0.34)	100.44(0.40)
			22	Egg	0.70(0.02)	39.70(0.58)	49.90(0.78)	0.57(0.05)	90.87(1.30)
			13	St	0	2.89(0.10)	96.08(0.99)	0	98.97(1.05)
			1	Melt	21.74	7.35	15.87	14.41	59.37
		1300	24	PhD	17.82(0.52)	16.18(1.14)	45.60(1.06)	7.13(0.20)	86.73(1.03)
Pyrolite	21	1500	21	Gt	29.50(0.28)	15.08(1.08)	48.03(0.68)	7.67(0.34)	100.27(0.58)
			15	St	0	0.68(0.46)	100.36(0.48)	0	101.04(0.83)
		1300*	31	PhD	20.19(0.50)	4.94(0.75)	56.83(0.81)	5.48(0.22)	87.44(1.24)
			17	Fe ₂ O ₃	6.23(0.99)	0.36(0.08)	0.68(0.49)	92.36(2.53)	99.63(1.07)

Figure S1

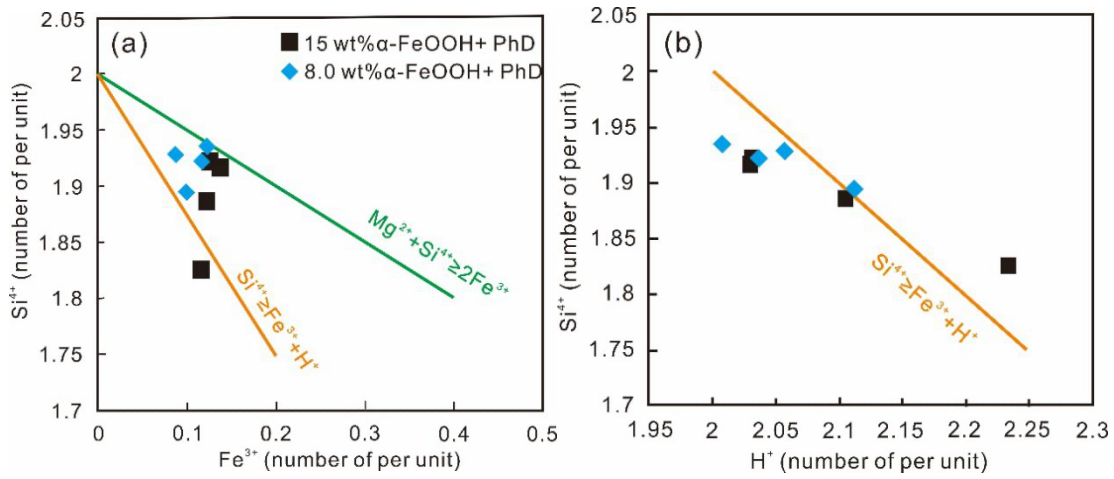


Figure S1. The Fe^{3+} substitution mechanism in PhD determined from chemical composition. (a) Si abundance as a function of Fe^{3+} abundance and (b) Si abundance as a function of H^+ abundance.